Review Paper:

An overview on spray pyrolysis deposition of metal oxide thin films

Soonmin Ho[1*] and Naser Ahmed[2]
1. Faculty of Health and Life Sciences, INTI International University, Putra Nilai,71800, Negeri Sembilan, MALAYSIA
2. School of Physics, Universiti Sains Malaysia, 11800, Penang, MALAYSIA
*soonmin.ho@newinti.edu.my

Abstract

This work provided an overview on the synthesis of metal oxide thin films on different types of substrates (soda lime glass, fluorine-doped tin oxide glass, silica glass, stainless steel, quartz, silicon and microscopic glass slide) using spray pyrolysis method. The fundamentals, advantages and limitations of this method have been described. Experimental results indicated that the properties of films were strongly depending on the specific process parameters (nozzle type, distance between nozzle and substrate, solvent type, solution flow rate, precursor concentration, compressed air pressure, spray time and substrate temperature).

It was noted that deposition temperature could control the surface chemical composition based on the experimental results. The presence of amorphous or polycrystalline structure could be observed for the films prepared at different deposition times as indicated in XRD studies. The obtained films indicated excellent absorption coefficient value (10^4 to 10^5 cm^{-1}) and high transmittance value (more than 82 %) in the visible and infrared portion.

Keywords: Metal oxide, thin films, semiconductor, band gap, spray pyrolysis method.

Introduction

Metal oxide thin films were considered as promising materials for various applications such as smart windows, photocatalysts, electrochromic devices, photovoltaic devices[21], batteries, anti-ferromagnetic materials, chemical capacitor and gas sensor[22]. These films showed direct band gap value, excellent absorption co-efficient value[26], high transmittance value, excellent chemical and thermal stability[13].

Thin films have been prepared using physical deposition method and chemical deposition technique. The structural properties of nanomaterials (particle shape, size and porosity) are greatly influenced by the synthetic procedures and conditions of the process[25]. Spray pyrolysis is a method that deposits a nanoparticle by spraying a precursor solution onto a heated surface[31]. The liquid precursor must be atomized under a specific pressure before becoming a fine mist. Using nitrogen or argon gas, the precursor solution is broken up into tiny droplets. These droplets hit the heated substrate, react chemically and leave behind a thin layer of material[45].

A wide range of materials can be deposited using spray pyrolysis technique including semiconductors materials, noble metals, ceramics materials, biomedical materials, various materials oxide and composites of different materials. This method became the most popular being cost-effective and efficient[51].

In this study, synthesis of metal oxide films using spray pyrolysis method has been reported. The properties of prepared films were investigated via different tools (XRD, EDX, SEM, AFM, XPS, TEM, UV-visible spectrophotometer and Raman spectroscopy).

Fundamentals, advantages and limitations of spray pyrolysis method: In the process of spray pyrolysis, clusters of liquid or vapour atoms from different chemical species undergo a thermally induced chemical reaction which results in the formation of tiny droplets of liquid[44]. It involves spraying an aqueous solution, usually one with soluble salts of the target molecule's atoms onto a heated surface. A single crystal or a collection of crystallites is created because of every droplet's pyrolytic breakdown, once it reaches the surface of the hot substrate[34]. This deposition method has advantages like low-cost[9], simple equipment, continuous and single-step process[6] to produce thin films (generally spherical morphology and uniform size). Deposition process could be carried out in open atmosphere conditions and did not require high quality reagents.

Spray pyrolysis has some restrictions and limitations like any other method. The spray pyrolysis procedure is highly dependent on several variables[43] including temperature of the substrate, nozzle to substrate distance, carrier gas flow rate and nozzle diameter. The film cracks at lower temperature while the film becomes rougher and more porous[17] at higher temperature. On the other hand, the initial droplet in a conventional spray pyrolysis has a diameter of around 5 microns.

However, we require droplets that are much smaller in size and the solution type content to produce nanoparticles. The spray pyrolysis method involves a lot of factors[7] that could have an impact on the final product, making it quite empirical (the final product's uniformity, particle size and shape may be changed).

Metal oxide thin films

Stannic oxide (SnO_2) thin films[27] have been synthesized using 0.1M of tin chloride pentahydrate and compressed air (figure 1) in specific conditions (nozzle-substrate distance=25 cm, solvent=distilled water, solution flow rate=4mL/minute and substrate temperature=250 °C). The obtained films were studied using Field Emission Scanning electron microscope (nanoparticles with pores), X-ray diffraction (cassiterite phase with crystallite size about 29.92 nm), Energy dispersive X-ray (28.25% of tin and 71.75% of oxygen) and UV-visible spectroscopy (band gap of 3.54 eV). The effects of solvents on the properties of films were investigated[1]. The films synthesized using alcoholic solvents (methanol, ethanol, isopropanol and 1-propanol) showed higher crystalline phase, nanostructured morphology, higher optical transmittance (more than 75%) in visible portions and strong UV and violet emission.

The films prepared using water and hydrogen peroxide showed very weak UV and violet emission peaks, lower optical transmittance value and mat-like morphology. On the other hand, ultrasonic spray pyrolysis method has been used to prepare thin films[24]. Based on the SEM analysis, film thickness and mean grain size were observed to be 80-2690 nm and 50-325 nm respectively. Kameswara and Vinni[28] proposed that high speed growth of thin films could be conducted via spray pyrolysis method. The obtained films showed homogeneous morphology, excellent optical transmission (more than 82 %), stronger diffraction intensity along (200) direction and sheet resistance of 35 ohms per square.

Aluminium oxide (Al_2O_3) films could be used in micro-electronic devices and opto electronic devices. These films showed thermal and chemical stability, high dielectric constant and excellent adhesion to many surfaces. Al_2O_3 films have been synthesized on quartz substrates[5] using aluminium acetyl acetonate (in ethanol). The optical transparency and band gap value increased, but particle size reduced (27 to 14 nm) when the temperature was increased (500°C to 700 °C). Fourier Transform Infrared Spectroscopy (FTIR) and X-ray photoelectron spectroscopy (XPS) studies confirmed the presence of chemisorbed oxygen in the obtained samples.

Frutis and co-workers[18] have prepared films onto silicon substrate using aluminium acetylacetonate (N, N-dimethylformamide). The band gap, activation energy, dielectric constant and interface states density were found to be 5.63 eV, 31 kJ/mol, 7.9 and 10^{11}X 1/eV.cm^2) respectively. On the other hand, thin films with high deposition rate (7 to 11.4 nm/minute) could be synthesized[41] at lower temperature (350 °C). The refractive index and destructive breakdown electric field were 1.645 and 6 MV/cm respectively. The density of interface states was 1.6 x10^{11} (eVcm^2)$^{-1}$ based on the quasistatic and high frequency C-V studies. The crystalline films prepared with (two-face nature) and without the addition of water mist (amorphous phase) have been studied using transmission electron microscopy[19].

In addition, hexagonal structure with specific cell lattice constants (a=0.5575 nm and c=0.876 nm) was reported. The superhydrophobic surface was generated[12] using alcohol solvents (ethanol, methanol and 2-propanol) and modifying agents (stearic acid and palmitic acid). Experimental findings showed stability increased when the carbon chain was increased (alcohol and fatty acid). The water contact angle was 160° using stearic acid and 2-propanol solution.

Nickel oxide films have been employed as chemical sensors, smart windows, photocatalysts, batteries, anti-ferromagnetic materials and electrochromic display devices. These p-type conductivity materials showed good chemical stability and excellent magnetic properties. The NiO films[47] have been produced onto microscopic glass slide (substrate) using nickel nitrate hexahydrate and nitric acid (stabilizer). Based on the SEM images, different morphologies could be observed for the films deposited using 0.015 M (starts to grow), 0.03 M (showed discontinued microplots on the surface), 0.04 M (well covered the surface of substrate), 0.05 M (completely covered) and 0.1 M (micro agglomeration observed) precursor concentration.

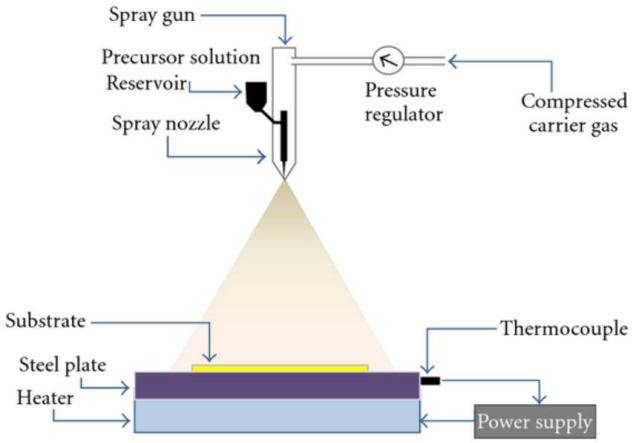

Figure 1: Scheme of the chemical spray pyrolysis method setup[27]

Table 1
Properties of the nickel oxide films synthesized using various precursor concentrations[47]

Precursor concentration (M)	Band gap (eV)	Thickness (nm)	Average transmittance (%)	Lattice constants (nm)	Grain size (nm)
0.015	3.68	181.57	88.3	--	--
0.03	3.62	191.66	71.01	0.4160	15.207
0.04	3.6	170.36	57.56	0.4163	20.275
0.05	3.64	190.34	64.28	0.4153	18.552
0.1	3.56	200.00	51.66	0.4165	37.085

Other properties of the obtained samples (band gap, thickness, grains size, lattice constants and transmittance value) have been highlighted in table 1. Zengjun and co-workers[52] have demonstrated the production of films onto soda lime glass using nickel (II) acetate tetrahydrate solution. According to Raman spectra, both samples showed similar Raman bands at 500 cm^{-1} and 1095 cm^{-1}. In the XRD studies, three major diffraction peaks (2θ=37.47°, 43.26° and 62.67°) could be observed and crystallite size increased (4 to 10 nm) when the deposition temperature was increased (300 to 420 °C) for the films prepared from aqueous solutions. However, the films produced in alcoholic solution indicated weak reflection and amorphous phase.

Based on the XPS investigations, $Ni(OH)_2$ and hydroxyl group disappeared when the deposition temperature was increased. It was noted that deposition temperature could control the surface chemical composition effectively. The electrochemical properties of the obtained films (precursor concentration=0.025 M, solution flow rate=1.5 mL/minute, compressed air pressure=0.5 bar, spray time=8 minutes, substrate temperature=450 °C, nozzle-substrate distance=40 cm) in alkaline electrolyte were reported[10].

Based on the XRD studies, three diffraction peaks (2θ=37.26°, 43.31° and 79.36°) could be observed. Additionally, two peaks (550 and 1100 cm^{-1}) could be observed in Raman analysis and porous structure was detected in the SEM image. In the cyclic voltammetry (CV) curves, current density increased when the scan rate was increased (5 to 20 mV/s). Furthermore, small separation between redox peaks showed rapid electron transfer properties. Experimental findings confirmed that the highest specific capacitance was 24 F/g (scan rate=5 mV/s, 1M KOH).

Iron oxide film could be used in gas sensor due to wide band gap value, high refractive index, chemical stability, greater porosity structure and smaller particle size. It was noted that physical deposition method (chemical vapor deposition and laser-assisted chemical vapor deposition) could produce good quality films. However, there exists lack of flexibility and cost effectiveness. Therefore, the chemical deposition method (spray pyrolysis, dip coating and spin coating) was simple and cost-effective technique. The Fe_2O_3 films have been deposited onto glass slide[3] using $Fe(NO_3)_3.9H_2O$ using distilled water in specific conditions (nozzle diameter=0.7mm, spraying process =lasted for 15 seconds, height of spraying nozzle=35 cm, solution molarity=0.1M, rate of spray process=10 cm^3/minute). A thinner layer (76 to 94 nm) with amorphous phase was formed when the deposition time was 5 minutes.

Thicker layer was (42 to 564 nm) produced when the deposition time was 40 minutes. Iron chloride is starting material for the synthesis of films[14]. XRD studies highlighted that amorphous phase and polycrystalline structure (major orientation along (104) direction) could be formed when the substrate temperature was less than 450 °C and at 500 °C respectively. SEM images confirmed homogeneous uniform and grain size of 19-25 nm. The prepared films indicated good transmittance value (80%) in visible and infrared portion. The influence of substrate temperature (250 to 450 °C) on the properties of films was studied[20]. Film thickness (360 to 190 nm) and electron-phonon interaction (4.089 to 1.778) reduced, but direct band gap (2.1 to 2.39 eV), refractive index (2.49 to 2.87) and indirect band gap (1.87 to 1.99 eV) increased when the substrate temperature was increased.

Optical investigations showed that absorption edge moved toward lower wavelength by increasing the substrate temperature. The absorption coefficients were observed in the range of 10^4 to 10^5 cm^{-1} and absorption index was 10^{-2} (light energy lost through scattering process). The $FeCl_3.6H_2O$ was used as precursor[42] during the preparation of films in highlighted conditions (substrate temperature=350 °C, distance between substrate and nozzle=50 cm, jet flow rate=5 mL/minute, spraying time=30 minutes, gas vector=nitrogen). The formation of amorphous phase (rust red in color) could be detected in as-deposited films. However, well-crystalline structure could be observed in annealed films (in vacuum sealed tube, 10^{-4} Pa, 5 hours, 350 °C). Other properties were investigated using SEM (granular, compact, grain size of 50nm to 200 nm) and UV-visible (band gap=2.1 eV) spectrophotometer.

Quartz has been used as substrate[48] during the preparation of thin films in the specific conditions (spray mode=ultrasonic nebulizer, air blast=atomizer, ultrasonic frequency=1.67 MHz, droplet size=2.89 μm, solution flow rate=10 mL/hour, distance from heater to substrate=5 cm, solvent=methanol and distilled water). According to XRD studies, different structures could be identified when the substrate temperature

was 400 °C (amorphous phase), 500 °C (crystalline phase), 600 °C (mixed phase: magnetite and hematite) and 700 °C (hematite). It was noted that needle type, granular type and plate type morphology could be found in the films prepared at temperature of 500, 600 and 700 °C respectively.

The surface roughness increased (16.62 to 36.27 nm) by increasing the temperature. According to transmittance spectra, the highest transmittance (55% in visible range) could be detected when the temperature was 500 °C. Lower transmittance value was due to light scattering (defect state and rough surface).

Magnesium oxide (MgO) is a highly ionic crystalline solid. The lattice constant, refractive index and dielectric constant were 0.421 nm, 1.736 and 10 respectively. This material could be used in microwave device (low dielectric loss) and optical waveguide films (low refractive index). Magnesium nitrate was used as precursor[33] to produce thin films on stainless steel substrate in highlighted conditions (substrate temperature=673 K, carrier gas=air, nozzle diameter=0.2 mm, distance between substrate surface and nozzle=30 cm, spraying rate=2 mL/minute). The obtained cubic phase structure showed crystallite size of 174 nm, hydrophilic nature and contact angle of 22°.

Several FTIR bands could be found such as 534.08 cm^{-1} (Mg-O stretching vibration), 1415.17 cm^{-1} (OH stretching mode in water compound) and 3441 cm^{-1} (surface adsorbed OH group). In the cyclic voltametric investigation, specific capacitance reduced (202.36 to 77.51 F/g) when the scan rate was increased (5 to 100 mV/s) due to the insufficient growth. Based on the electrochemical impedance spectroscopy, charge transfer resistance and electrochemical series resistance were 0.35 Ω and 2.34 Ω respectively.

Additionally, electrochemical cycling stability showed 34 % stability over 1000 cycles. Diachenko and co-workers[16] have reported the production of films on glass slide using 0.2 M magnesium chloride in specific conditions (air flow pressure=0.2 MPa, nozzle diameter=0.2 mm, distance between substrate surface and nozzle=15cm, substrate temperature=640 to 690 K). The obtained results showed film thickness (0.8 to 2.2 μm) and transmittance value increased when the substrate temperature was increased.

Moses and co-workers[36] have reported the synthesis of films onto quartz substrate (400 and 600 °C) using 0.15 M of magnesium acetate. Optimized deposition conditions (volume of precursor sprayed=50 mL, solvent=90% ethanol+10% tri-ethylene glycol, spray rate=5 mL/minutes, carrier gas pressure=0.4 kg/cm^2) have been stated and MgO film growth mechanism was highlighted.

Based on the thermogravimetry analysis (TGA) and differential thermal analysis (DTA), three stages could be observed at 61°C-168 °C (removal of physiosorbed water), 168 °C-346°C (decomposition of $Mg(CH_3COO)_2$) and 500 °C (formation of magnesium oxide).

In the XRD studies, crystallite size, dislocation density, strain and number of crystallites were observed to be 30.12-34.12 nm, 1.1-0.879 $X10^{11}$ lines/cm^2, 1.16-0.75, 0.973-0.206 $x10^{10}/cm^3$ respectively when the temperature was increased from 500 to 600 °C. Further, experimental results confirmed that both films were transparent in the visible and infrared range. However, higher transparency (more than 80 %) and larger band gap value (5.25 eV) could be found when the films were produced at 600 °C.

$$Mg(CH_3COO)_2.4H_2O \rightarrow Mg(CH_3COO)_2 + 4H_2O$$
$$Mg(CH_3COO)_2 \rightarrow MgCO_3 + (CH_3)_2.CO(g)$$
$$MgCO_3 \rightarrow MgO + CO_2(g)$$

Solvent mixed spray pyrolysis technique (magnesium nitrate and hexa methylene tetramine) has been used to prepare thin films onto SiO_2 substrate[38]. Characterization of the obtained films has been carried out using transmission electron microcopy (small amount of agglomeration happened as shown in figure 2), XRD (cubic structure, crystallite size=9.2 nm, lattice parameter (a=b=c=0.4213 nm)) and UV-visible spectrophotometer (band gap=4.2 eV). It was noted that optical conductivity (200-400 nm) and extinction coefficient (400-1100 nm) increased during the experiment. The influence of temperature on the properties of films was studied[40].

The band gap (3.38 to 3.7 eV), average surface roughness (12.2 to 26.2 nm), film thickness (85.3 to 119.5 nm), roof mean square roughness (15.6 to 33.7 nm), micro strain ($1.89x10^3$ to $4.35x10^3$) and crystallite size (200 to 1000 nm) were varied when the temperature was increased (643 to 693 K). Based on the photoluminescence analysis, two peaks could be observed at 412 nm (3 eV) and 524 nm (2.38 eV) contributing to the hole trapped on magnesium ions vacancy and the presence of defects with oxygen ion vacancy.

Tungsten oxide nanostructured films have been used in gas sensor, switchable mirror and electrochromic windows. These n-type materials were non-toxic, wide band gap value, excellent intercalation properties and have a rapid response time. The WO_3 films have grown onto fluorine doped tin oxide glass[37] in specific conditions (distance between substrate and the spray gun=30 cm, temperature=250 °C, tungstic acid=precursor). Based on the optical studies, thicker films formed when the precursor volume increased (resulted in transmittance will be reduced). All the obtained films showed electrochromic properties. The highest coloration efficiency was 52.27 cm^2/C (5mL) followed by 36.64 cm^2/C (10 mL) and 29.38 cm^2/C (15 mL) when the precursor concentration was 0.1 M (figure 3).

The coloration efficiency ((46.61 cm^2/C=5mL, 33.29 cm^2/C=10 mL, 28.67 cm^2/C=15 mL)) was observed slightly lower when the concentration of precursor was 0.05 M. SEM

studies exhibited wall-like structure with bubble-like islands, randomly distributed on the WO_3 granular background. The use of surfactants (hexadecyltrimethylammonium bromide (HTAB) and polyethylene glycol (PEG400):HTAB) as growth controlling agents could influence the properties of the films, nucleation and growth process[8]. Morphology studies indicated that different morphologies could be observed in the WO_3 sample by adding HTAB (homogeneous with low porosity) and by adding PEG (larger grain size). Experimental results showed that the electrochromic activity could be improved by using these agents. The coloration efficiency and optical modulation were found to be 31.5 cm^2/C and 38% respectively in the PEG-HTAB mixtures.

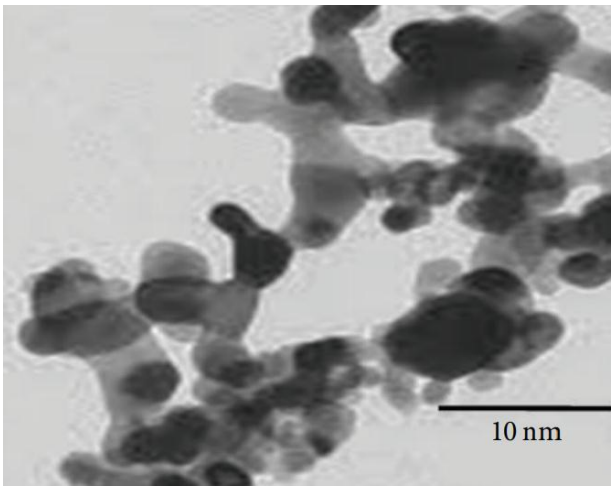

Figure 2: TEM image of the MgO films[38].

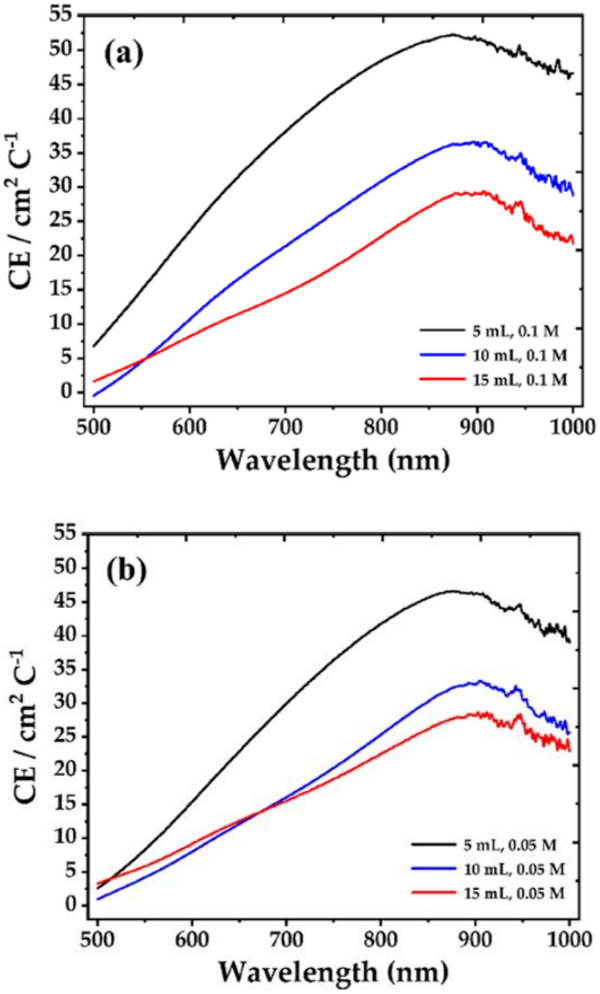

Figure 3: The coloration efficiency[37] of the samples (a) 5, 10 and 15 mL with 0.1 M precursor solution (b) 5, 10 and 15 mL with 0.05 M

The p-type copper oxide films could be used in photovoltaic applications due to suitable band gap value (1.2 to 2.1 eV), excellent absorption coefficient (10^5 cm^{-1}, at 300 K), good electrical resistance (10 to 10^5 Ω.cm) and excellent thermal conductivity (76.5 W.m/K). Synthesis of films was produced onto glass slide using copper acetate, 2-propanol and glucose[30]. The prepared films showed reddish yellow color, composed of rounded grain (about 50 nm), surface roughness of 30 nm, direct band gap of 2.6 eV and indirect band gap of 1.95 eV.

On the other hand, the influence of substrate temperature[15] on the properties of films was reported (using same starting material). XRD results showed high purity, single CuO phase with monoclinic structure in the specific conditions (nozzle diameter=0.2mm, substrate temperature= 600K to 725 K, distance between nozzle and substrate surface=17cm, spraying rate=2 cm^3/min, volume of sprayed solution=5 cm^3). Three peaks at 268 cm^{-1} (A_{1g} mode), 320 cm^{-1} (B_{1g} mode) and 604 cm^{-1} (B_{2g} mode) could be observed in Raman spectra. AFM analysis indicated homogeneous surface with tightly packed grains, grain size increased when the substrate temperature was increased (figure 4).

It was noted that coherent scattering domain increases (23.1 to 24.1 nm) when the temperature was increased (600 K to 650 K) and then dropped (21 nm) at temperature of 725 K. The average arithmetic roughness (R_a) and root mean square deviation from the mean line (R_q) were determined according to the AFM technique. R_a (15.51 to 46.08 nm) and R_q value (18.69 to 58.12 nm) increased by increasing the temperature (600 K to 650 K).

Further increase in substrate temperature caused R_a (19.3 nm) and R_q (25.36 nm) reduced. Thin films have been synthesized using 0.05 M $CuCl_2.2H_2O$ (150 mL) in deionized water at various temperatures[29]. Experimental results showed that film thickness (1.02 to 0.43 µm), macro strain ($7.22x10^{-3}$ to $1.85x10^{-3}$), lattice parameters (0.43018 to 0.42788 nm), volume of unit cell (0.0796 to 0.0783 nm^3) reduced, when the temperature was increased (200 to 350 °C). It was noted that all the films showed high transmittance values (850-1100 nm) and high reflection value (visible portions) based on the optical analyses. The influence of precursor concentration on the CuO films was reported[50].

The precursor is produced by dissolving cupric acetate in distilled water (50 mL) stirred for 30 minutes at room temperature. XRD studies indicated that better crystallinity (tenorite phase) could be observed at higher concentration of precursor. Based on the SEM images, the films prepared using 0.05 M showed very fine with no distinct boundaries while irregular nanospheres with inconsistent growth could be observed by using 0.1M concentration.

In the optical investigations, the films produced using lower concentration indicated higher transparency (80 %) in the visible region if compared to the films produced using 0.1 M (less than 20 %). Other results such as resistance, thickness, band gap and crystallite size have been highlighted in table 2.

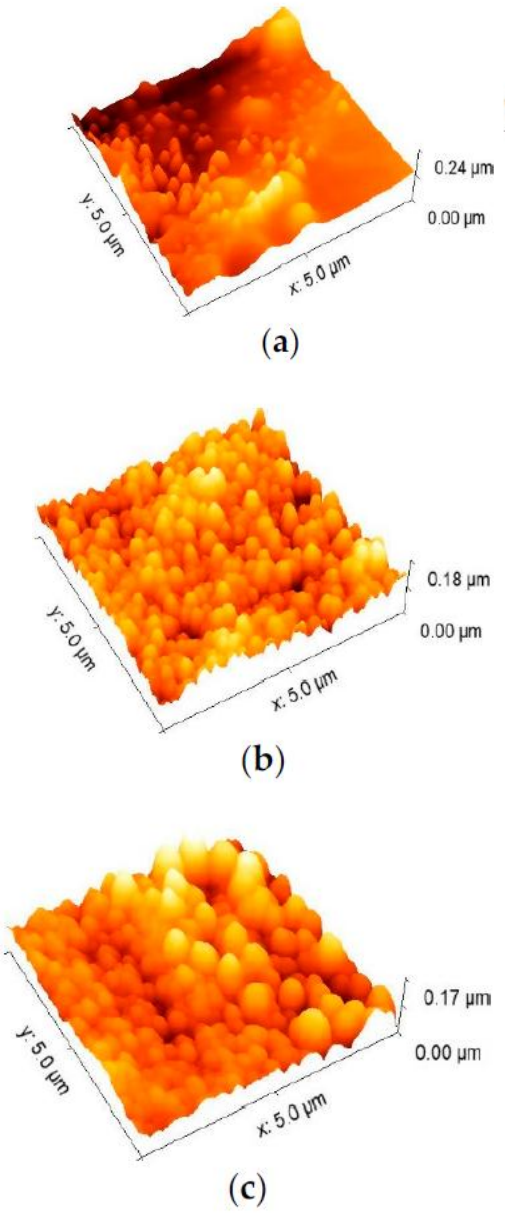

Figure 4: The AFM images (3-dimensional) of the films prepared in different substrate temperatures[15]. (a) 625k (b) 675K (c)725K

Table 2
Properties of the CuO films.

Sample	Crystallite size (nm)	Band gap (eV)	Thickness (nm)	Resistance
0.05 M	10.5	1.52	320	9.8 GΩ
0.1 M	16	1.56	590	1.18 MΩ

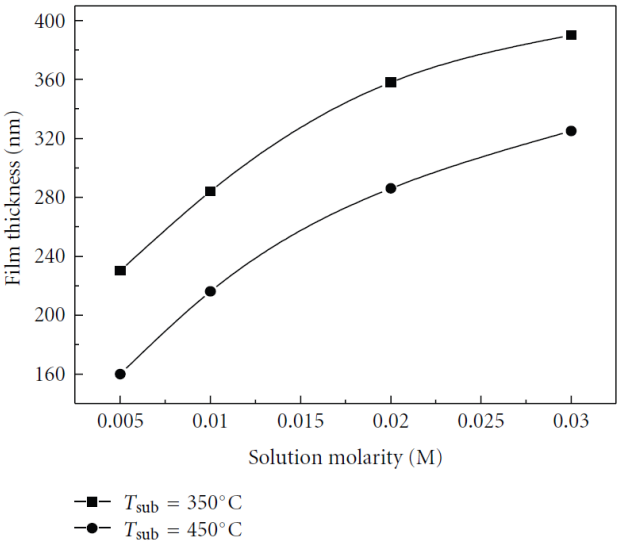

Figure 5: Film thickness versus solution molarity produced at different substrate temperatures[2]

Iridium oxide films have attracted considerable interest due to their physical, chemical and electro chemical properties. These materials could be employed in electrochromic devices, gas sensor, smart window and thermal control devices. Several deposition techniques (pulsed laser deposition, liquid delivery metal organic method, sputtering technique and thermal evaporation) have been used to produce thin films. However, these deposition techniques were expensive for industrial applications. The deposition process was conducted onto glass slides using iridium chloride[2].

The obtained films showed blackish, uniform morphology and excellent adherent to the substrate. Figure 5 showed that thicker films could be produced when the temperature was 350 °C. When the temperature was increased to 450 °C, thickness reduced (higher evaporation rate). XRD studies revealed that amorphous phase and poly crystalline (tetragonal structure) could be found when the temperature was 350 °C and 450 °C respectively. Several diffraction peaks such as (110), (101), (200) and (211) perfectly matched with ICDD (number: 15-870). Dark electrical conductivity of films was studied. Lower value of electrical conductivity in the amorphous phase was compared to polycrystalline structure. Electrical conductivity increases (15.9 to 23.8 $\Omega^{-1}.cm^{-1}$) when the solution concentration was increased (0.005 M to 0.03 M) in both substrate temperatures.

$$2IrCl_3 + 3H_2O \rightarrow 6HCl + Ir_2O_3$$
$$Ir_2O_3 + \frac{1}{2}O_2 \rightarrow 2IrO_2$$

Manganese oxide films existed in different phases (MnO, Mn_3O_4, MnO_2 and Mn_2O_3) due to various oxidation numbers (Mn^{2+}, Mn^{4+} and Mn^{3+}). These films could be used in sensor, battery, solar energy conversion, magneto electronic devices, electro chemical capacitor and electro chemical energy storage devices. Deposition of tetragonal phase of Mn_3O_4 films[11] onto glass substrate using manganese chloride was observed (figure 6). XPS investigations highlighted several peaks found at 529 eV (O, 1s), 640.4 eV (Mn, 2p3/2) and 652.4 eV (Mn, 2p1/2). Lattice parameter (a=b=0.5764, c=0.9475), defect density ($1.6119x10^{-3}$) and crystallite size (24.9075 nm) were reported based on XRD studies.

Topography analysis was carried out using tapping mode (scan area=2 µm X 2µm) and it showed porous nanoflakes (egg shaped) and surface rms roughness as 50 nm. Optical measurement revealed very low transmittance value (15% to 30%) due to inhomogeneity surface. The growth of cubic phase of MnO films onto glass substrates in the specific conditions was observed (purified air=carrier gas, constant flow rate=3 mL/min, distance between substrate and nozzle=30 cm)[49]. The photoluminescence (PL) emission intensity increases when the temperature was increased (350 °C to 400 °C). In addition, the obtained films excited at 389 nm, while two peaks could be observed (485 nm and 531 nm) in PL spectra. The transmittance spectra indicated 10% of increase in transmittance value for the films prepared at 400 °C if compared to 350 °C.

Jadhav and workers[23] suggested that the best deposition temperature was 400 °C also. The prepared films showed tetragonal structure with (301) orientation and average grain size was 70nm. SEM and AFM indicated a high degree of porosity and rougher surface respectively. The specific capacitance (527 F/g, 1M NaSO, scan rate=5 mV/s), specific energy (6.52 Wh/kg), specific power (4.5 kW/kg) and coulomb efficiency (89.94%) were reported. Synthesis of hausmannite phase of Mn_3O_4 films on pyrex glass slides[35] using 0.15 M manganese acetate in ethyl alcohol solution (volume of precursor=50 mL, substrate temperature=350 °C to 450 °C, spray rate=5 mL/min, carrier gas pressure=0.4 kg/cm^2, distance between nozzle and substrate=30 cm, carrier gas=air).

In the thermogravimetry analysis, thermal decomposition could be observed in different temperature range such as 50 °C-120 °C (loss of 4 mol of water per mol of salt), 120-129 °C (formation of manganese oxyacetate), 270-320 °C (formation of manganese oxide) and at above 490 °C (formation of Mn_2O_3). According to XRD data, lattice parameter (a=b=0.5752, c=0.947) and unit cell volume (0.31336 nm^3) were determined for the films prepared at 400 °C. Furthermore, crystallite size, dislocation density, micro strain and the number of crystallites/unit area were found to be 49.42 nm, $4.91x10^{14}/m^2$, $5.29x10^{-3}$ and $3.86X10^{15}$ respectively.

Zinc oxide films were classified as II-IV semiconductors. These materials could be used in transistors, sensor, solar cell, piezoelectric devices and photodetector. The prepared films indicated excellent magnetic, electrical, optical, catalytic and gas-sensing behaviors. Thin films[4] were deposited onto various types of substrates [glass and single crystalline (100) oriented silicon] using zinc nitrate. Film thickness and band gap were found to be 50 nm-500 nm and 3.26-3.3 eV respectively. The prepared films indicated high electrical resistance (greater than 1 MΩ) and displayed long time relaxation of photoelectrical response (up to 10 minutes). Krunks and co-workers[32] have synthesized films on glass substrate at temperature of 670 K. The obtained films showed the most intense diffraction peak in (002) direction and exciton emission band at 8K (photoluminescence spectrum).

Grain size was found to be 50 nm to 400 nm and exhibited high optical transmittance value. Zinc acetate dihydrate, monoethanolamine and soda lime glass[46] were used as zinc precursor, stabilizing agent and the substrate for the ZnO preparation (nozzle caliber=0.5 mm, aluminum alloy cup=25 mL, spray width=50 mm, gun to substrate distances=20 cm, 30 cm). According to XRD analysis, better crystallinity could be observed for the films prepared with 2 mL solution (due to more ZnO coating). Additionally, these films showed more defined structures, uniform in size (40 nm to 50 nm) and very little agglomeration. When the photoactivity was conducted (degradation of rhodamine B dye), the sample showed the best degradation efficiency. The spray pyrolysis setup (figure 7) was highlighted and mechanism was proposed as follows:

$$ZnO + hv \rightarrow h^+ + e^-$$

$$h^+ + OH^-/H_2O \rightarrow \cdot OH$$

$$e^- + O_2 \rightarrow \cdot O_2^-$$

$$\cdot OH + dye\ molecules + \cdot O_2^- \rightarrow CO_2 + H_2O + inorganic\ acids$$

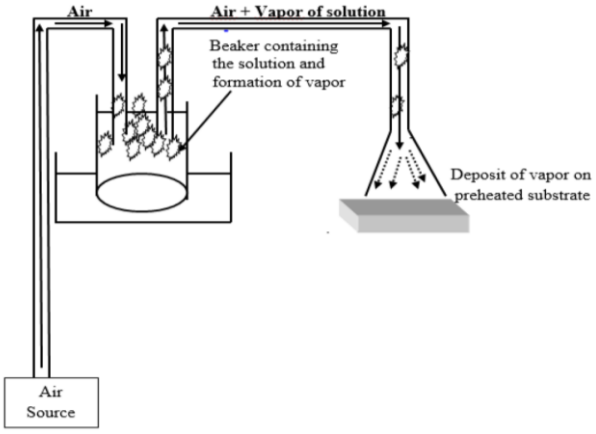

Figure 6: Schematic diagram of the synthesis of thin films using spray pyrolysis method[9].

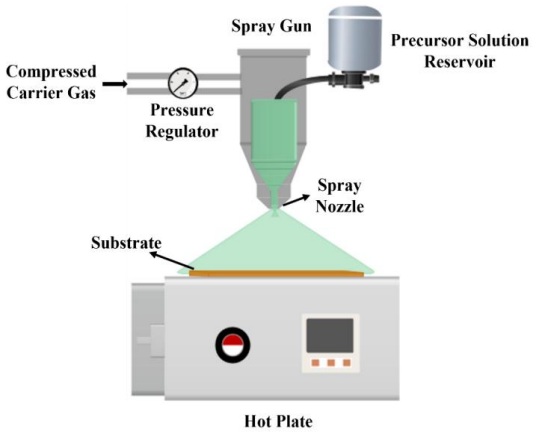

Figure 7: Schematic of the spray pyrolysis setup[46].

Nora and Bizarro[39] have reported the influence of precursor solution on the properties of films (distance between substrate and nozzle=30 cm, substrate=corning glass slide, substrate temperature=450 °C, gas flow rate=1024 mL/min, solution flow rate=3.7 mL/min, precursor=zinc acetate). Characterization of the obtained films was reported (nanoflake morphology, reaction rate of 0.0121 min^{-1}, surface-to-volume ratio of 0.061 n/m, band gap of 3.23 eV, surface roughness of 48-153 nm, thickness of 210-851 nm and grain size of 37-42 nm). Decomposition reaction could produce zinc oxide and many side products (carbon dioxide, acetic acid and acetone). These side products were very volatile and resulted in the zinc ions reacting with oxygen to produce the oxide.

In addition, decomposition reaction will form hydrochloric acid (HCl) for both water and methanol. HCl caused chemical etching of the surface of the substrate and thus, poor surface morphology was observed.

$$Zn(CH_3CO_2)_2.2H_2O \rightarrow ZnO + CO_2, CH_3CO_2H, CH_3COCH_3$$

$$ZnCl_2 + H_2O \rightarrow ZnO + 2HCl$$

$$2ZnCl_2 + CH_3OH + \frac{3}{2}O_2 \rightarrow 2ZnO + 4HCl + CO_2$$

On the other hand, zinc chloride was used to produce thin films and the experimental results were highlighted (nanorod morphology, reaction rate of 0.0079 min^{-1}, surface-to-volume ratio of 0.035 n/m, band gap of 3.23 eV, roughness of 84-163 nm, thickness of 335-719 nm and grain size of 44-46 nm).

Conclusion

Spray pyrolysis method has been used to synthesize metal oxide films. In this work, the properties of tin oxide, aluminium oxide, nickel oxide, iron oxide, magnesium oxide, tungsten oxide, copper oxide, iridium oxide, manganese oxide and zinc oxide were studied. The prepared nanostructured films could be used in photovoltaic devices, microwave devices and optical waveguide materials because of wide band gap value (1.2 eV to 5.63 eV), excellent transmittance value (more than 82 %) and high absorption coefficient value (10^4 to 10^5 cm^{-1}).

Acknowledgement

This research work was supported by INTI International University (Ho SM).

References

1. Abdul P. and Bushiri M., The effect of solvents on the growth and key properties of tin oxide thin films deposited via chemical spray pyrolysis, *Mater. Chem. Phys.*, https://doi.org/10.1016/j.matchemphys.2020.124209 **(2021)**

2. Akl A., Mahmoud A. and Shomar S., Electrical Characteristics and Nanocrystalline Formation of Sprayed Iridium Oxide Thin Films, *Adv. Condens. Matter Phys*., doi:10.1155/2010/518209 **(2010)**

3. Alaa A., Optical properties of crystalline and non-crystalline iron oxide thin films deposited by spray pyrolysis, *Appl. Surf. Sci*., **233**, 307–319 **(2004)**

4. Andrzej M., Sagan P., Kuzma M. and Popovych V., Zinc oxide films prepared by spray pyrolysis, *EPJ Web Conf*., https://doi.org/10.1051/epjconf/201713303004 **(2017)**

5. Baban P., Tom M., Dash S. and Tripura S., Spray pyrolytic deposition of transparent aluminum oxide (Al_2O_3) films, *Appl. Surf. Sci.*, **258**, 1091-1096 **(2011)**

6. Balakarthikeyan R., Sayed Z., Mohammad S., Mohd U. and Ahmed A., Enhancing the optoelectronic properties of low-cost nebulizer spray pyrolysis (NSP) prepared ZnS thin film through praseodymium doping for photodetector applications, *Mater. Sci. Eng. B*, https://doi.org/10.1016/j.mseb.2022.116213 **(2023)**

7. Bashir Y., Roslan H. and Halim M., The role of pH solution in depositing MoO_3 film by spray pyrolysis as hole selective contact on silicon-based heterojunction devices, *Results Phys.*, **45**, https://doi.org/10.1016/j.rinp.2023.106229 **(2023)**

8. Bertus L., Faure C., Danine A. and Labrugere C., Synthesis and characterization of WO_3 thin films by surfactant assisted spray pyrolysis for electrochromic applications, *Mater. Chem. Phys.*, **140**, 49-59 **(2013)**

9. Bouachri M., Carlos D., Paloma F., Fahoume M. and Ouannou A., Substrate temperature effects on the structural, morphological and optical properties of Bi_2S_3 thin films deposited by spray pyrolysis: An experimental and first-principles study, *Opt. Mater*., https://doi.org/10.1016/j.optmat.2022.113215 **(2023).**

10. Brioual B., Zaid R., Aouni A. and Diani M., Electrochemical behavior of spray deposited nickel oxide (NiO) thin film in Alkaline electrolyte, E3S Web Conf., https://doi.org/10.1051/e3sconf/202233600045 **(2022)**

11. Dahamni M., Ghamnia M., Naceri S. and Bouadi A., Spray Pyrolysis Synthesis of Pure and Mg-Doped Manganese Oxide Thin Films, *Coatings*, **11**, https://doi.org/10.3390/coatings11050598 **(2021)**

12. Daneshmand H., Nouri F. and Rezaeinasab M., Deposition of Superhydrophobic Fatty Acid-Coated Al_2O_3 Films by Spray Pyrolysis Method: Effect of Dispersion Mediums on Morphology and Roughness of the Layer, *Prot. Met. Phys. Chem. Surf.*, **57**, 335–343 **(2021)**

13. Das G., Tran T., Yoon H. and An S., Spherulitic copper–copper oxide nanostructure-based highly sensitive nonenzymatic glucose sensor, *Int. J. Nanomedicine*, **10**, 165-178 **(2015)**

14. Dghoughi L., Erguig H., Addou M. and Bernede C., Physico-chemical, optical and electrochemical properties of iron oxide thin films prepared by spray pyrolysis, *Appl. Surf. Sci.*, **253**, 1823-1829 **(2006)**

15. Diachenko O., Kováˇc J., Dobrozhan O., Novák P. and Skriniarova J., Structural and Optical Properties of CuO Thin Films

Synthesized Using Spray Pyrolysis Method, *Coatings*, https://doi.org/10.3390/coatings11111392 **(2021)**

16. Diachenko V., Opanasuyk A. and Kurbatov D., Oxide Films Obtained by Spray Pyrolysis Technique, 2016 IEEE 7th International Conference on Advanced Optoelectronics and Lasers (CAOL) conference proceedings: Odessa, Ukraine, 12-15 September 2016, Mechnikov National University, 31-33 **(2016)**

17. Exarhos G. and Zhou X., Discovery-based design of transparent conducting oxide films, *Thin Solid Films*, **515**, 7025-7052 **(2007)**

18. Frutis M., Garcia M. and Falcony C., Optical and electrical properties of aluminum oxide films deposited by spray pyrolysis, *Appl. Phys. Lett.*, https://doi.org/10.1063/1.121156 **(1998)**

19. Guzman J., Garcia M., Frutis M. and Falcony C., Structural characteristics of Al_2O_3 thin films prepared by spray pyrolysis, *J. Phys.: Condens. Matter*, DOI: 10.1088/0953-8984/13/50/101 **(2001)**

20. Hassanien A. and Alaa A., Optical characteristics of iron oxide thin films prepared by spray pyrolysis technique at different substrate temperatures, *Appl. Phys. A*, https://doi.org/10.1007/s00339-018-2180-6 **(2018)**

21. Ho S.M. and Emmanuel A., A short review of recent advances in copper oxide nanostructured thin films, *Res. J. Chem. Environ*., **23,** 138-145 **(2019)**

22. Ho S.M., A review of copper oxide thin films, *Int. J. Recent Sci. Res*., **7**, 11914-11918 **(2016)**

23. Jadhav P., More P., Patil V. and Ingole S., Preparation, structural and electrochemical super capacitive properties of sprayed manganese oxide film electrode, *J. Mater. Sci. Mater. Electron*, **28**, 707-714 **(2017)**

24. Jadsadapattarakul D., Euvananont C., Nukeaw J. and Sooknoi T., Tin oxide thin films deposited by ultrasonic spray pyrolysis, *Ceram. Int.*, **34**, 1051-1054 **(2008)**

25. Jin L., Zhixing W., Jiexi W., Guochun Y., Xinhai L. and Huajun G., Advances in nanostructures fabricated via spray pyrolysis and their applications in energy storage and conversion, *Chem. Soc. Rev.*, **48**, 3015-3072 **(2019)**

26. Jose M. and Lars O., Photodegradation of stearic acid adsorbed on copper oxide heterojunction thin films prepared by magnetron sputtering, *Chemengineering*, doi:10.3390/chemengineering 2030040 **(2018)**

27. Kajale D., Patil G., Jain H. and Gaikwad B., Spray pyrolysis deposition of nanostructured tin oxide thin films, *Int. Sch. Res. Notices*, https://doi.org/10.5402/2012/275872 **(2012)**

28. Kameswara L. and Vinni V., Novel mechanism for high-speed growth of transparent and conducting tin oxide thin films by spray pyrolysis, *Appl. Phys. Lett*., https://doi.org/10.1063/1.109964 **(1993)**

29. Kose S., Atay F., Bilgin V. and Akyuz I., Some physical properties of copper oxide films: The effect of substrate temperature, *Mater. Chem. Phys*., **111,** 351–358 **(2008)**

30. Kosugi T. and Shoji K., Novel Spray-Pyrolysis Deposition of Cuprous Oxide Thin Films, *J. Am. Ceram. Soc*., **81**, 3117-3124 **(1998)**

31. Kozhukharov S. and Tchaoushev S., Spray pyrolysis equipment for various applications, *J. Chem. Technol. Metall*., **48**, 111-118 **(2013)**

32. Krunks K., Bijakina O., Mikli V. and Varema T., Zinc oxide thin films by spray pyrolysis method, *Phys. Scr.*, DOI: 10.1238/Physica.Topical.079a00209 **(1999)**

33. Maheswary D., Sheeladevi C. and Johny Asir, Intestinal carriage of aminoglycoside resistant Enterococcus species among pediatric inpatients in a tertiary care hospital, *Res. J. Biotech*., **17(10)**, 26-31 **(2022)**

34. Mooney S. and Radding B., Spray pyrolysis processing, *Annu. Rev. Mater. Sci.*, **12**, 81-101 (**1982)**

35. Moses A., Grace V., Bena J. and Joachim W., XRD and XPS characterization of mixed valence Mn_3O_4 hausmannite thin films prepared by chemical spray pyrolysis technique, *Appl. Surf. Sci*., **256**, 2920–2926 **(2010)**

36. Moses A., Nehru C. and Sanjeeviraja C., Spray pyrolysis deposition and characterization of highly (100) oriented magnesium oxide thin films, *Cryst. Res. Technol.*, **42**, 867–875 **(2007)**

37. Mouratis K., Tudose I., Romanitan C., Pachiu C., Popescu M. and Simistiras G., WO_3 Films Grown by Spray Pyrolysis for Smart Windows Applications, *Coatings*, https://doi.org/10.3390/coatings12040545 **(2022)**

38. Nemade K. and Waghuley A., Synthesis of MgO Nanoparticles by Solvent Mixed Spray Pyrolysis Technique for Optical Investigation, *Int. J. Metals*, http://dx.doi.org/10.1155/2014/389416 **(2014)**

39. Nora S. and Bizarro M., Sprayed Pyrolyzed ZnO Films with Nanoflake and Nanorod Morphologies and Their Photocatalytic Activity, *J. Nanomaterials*, http://dx.doi.org/10.1155/2016/5981562 **(2016)**

40. Opanasuyk S., Diachenko O., Nam D. and Cheong H., Surface Morphology, Structural and Optical Properties of MgO Films Obtained by Spray Pyrolysis Technique, *Acta Phys. Pol. A*, **130**, 805-810 **(2016)**

41. Ortiz A. and Alonso J., High quality-low temperature aluminum oxide films deposited by ultrasonic spray pyrolysis, *J. Mater. Sci., Mater. Electron*, **13,** 7-11 **(2002)**

42. Ouertani B., Ouerfelli J., Saadoun M. and Ezzaouia H., Characterization of iron oxide thin films prepared from spray pyrolysis of iron trichloride-based aqueous solution, *Thin Solid Films*, **516**, 8584–8586 **(2008)**

43. Patil P., Versatility of chemical spray pyrolysis technique, *Mater. Chem. Phys*., **59**, 185-198 **(1999)**

44. Paulosutty A., Josue A., Bindu K., David A. and Shaji S., Sb_2S_3 thin films: from first principles to in situ crystalline thin film

growth by ultrasonic spray pyrolysis, *Mater. Sci. Semicond. Process*, https://doi.org/10.1016/j.mssp.2022.107269 **(2023)**

45. Perednis D. and Gauckler L., Thin Film Deposition Using Spray Pyrolysis, *J. Electroceram*., **14**, 103–111 **(2005)**

46. Rabeel M., Javed S., Khan R. and Akram M., Controlling the Wettability of ZnO Thin Films by Spray Pyrolysis for Photocatalytic Applications, *Materials*, https://doi.org/10.3390/ma15093364 **(2022)**

47. Rafia B., Boubaker B., Toufik S. and Rahal A., Effect of Precursor Concentration on Structural Optical and Electrical Properties of NiO Thin Films Prepared by Spray Pyrolysis, *J. Nanomaterials*, https://doi.org/10.1155/2017/5204639 **(2017)**

48. Rajendra N., Kaur D. and Pandey A., Growth and characterization of iron oxide nanocrystalline thin films via low-cost ultrasonic spray pyrolysis, *Mater. Chem. Phys*., **109**, 638–644 **(2009)**

49. Thirumalairajan S., Girija K., Sudha M. and Maadeswaran P., Structural and optical investigation of manganese oxide thin films by spray pyrolysis technique, *Optoelectron. Adv. Mater. Rapid Commun*., **2**, 779-781 **(2008)**

50. Vignesh S., John B., Shankar P. and Mani K., Growth and characterization of spray pyrolysis deposited copper oxide thin films: Influence of substrate and annealing temperatures, *J. Anal. Appl. Pyrolysis*, **111**, 272-277 **(2015)**

51. Vinay K. and Hridaya N., Versatility of spray pyrolysis technique for the deposition of carbon thin films, *J. Emerg. Technol. Innov. Res*., **4**, 312-318 **(2017)**

52. Zengjun C., Tatjana D., Acik O. and Malle K., Nickel oxide films by chemical spray: Effect of deposition temperature and solvent type on structural, optical and surface properties, *Appl. Surf. Sci*., https://doi.org/10.1016/j.apsusc.2021.149118 **(2021)**.

(Received 02nd February 2023, accepted 02nd April 2023)